ACS APPLIED NANO MATERIALS
Cite This: ACS Appl. Nano Mater. XXXX, XXX, XXX−XXX
Letter
www.acsanm.org

Pd Nanoparticle Catalysts Supported on Nitrogen-Functionalized Activated Carbon for Oxyanion Hydrogenation and Water Purification

Tao Ye,[†] Nathan A. Banek,[‡] David P. Durkin,[§] Maocong Hu,[∥] Xianqin Wang,[∥] Michael J. Wagner,[‡] and Danmeng Shuai*[,†]

[†]Department of Civil and Environmental Engineering, The George Washington University, Washington, D.C. 20052, United States
[‡]Department of Chemistry, The George Washington University, Washington, D.C. 20052, United States
[§]Department of Chemistry, United States Naval Academy, Annapolis, Maryland 21402, United States
[∥]Department of Chemical, Biological and Pharmaceutical Engineering, New Jersey Institute of Technology, Newark, New Jersey 07102, United States

Supporting Information

ABSTRACT: We provide an efficient, sustainable, low-cost, and potentially scalable method to prepare N-functionalized activated carbon (AC) for Pd-based catalysis with improved performance for water purification. N-functionalized AC supports were realized via "soft nitriding", that is, low temperature heating of a urea−AC mixture, and Pd nanoparticles with a significantly increased number of surface Pd(0) sites were achieved on the supports. Moreover, Pd nanoparticles were preferentially loaded near the (treated) AC exterior surface. N-functionalization improved nitrite and bromate hydrogenation kinetics but not for chlorite and chlorate, suggesting that different mechanisms determine the reaction activity of these oxyanions.

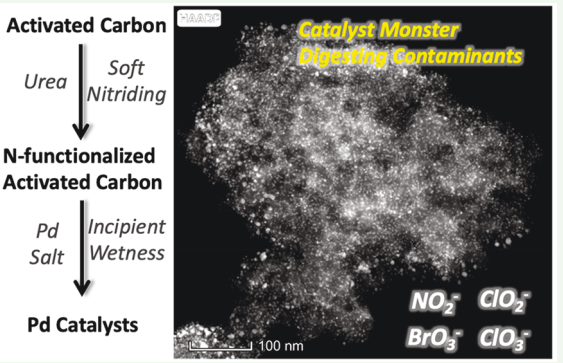

KEYWORDS: *palladium, nitrogen-functionalization, activated carbon, hydrogenation, water purification*

Catalyst supports have been found to significantly influence catalytic performance. Metal oxides, for example, Al_2O_3, SiO_2, and TiO_2, have been frequently used as catalyst supports. However, the application of metal oxide supports could be problematic because of the dissolution of the supports under acidic or basic conditions.[1,2] Carbon materials, such as activated carbon (AC),[2] carbon nanotubes (CNTs),[3] and carbon nanofibers (CNFs),[4,5] have been demonstrated to be excellent catalyst supports because of their chemical stability during reaction, high surface area and porosity, and adequate mechanical properties.[6] However, the high cost and difficulties of large-scale production limit the application of CNTs and CNFs.[3] Because of its low cost and wide availability, exceptionally high surface area and porosity, and ease of chemical modification, separation, regeneration, and recovery of immobilized noble metals, AC is the most used support for Pd-based catalysts for water purification.[2,7−10] The surface modification of AC (e.g., by O or N functional groups) was observed to increase Pd dispersion and optimize the catalytic activity.[2,6,9,11] However, strong acid treatment, high-temperature annealing, or pyrolysis for an extended period of time is required to produce a significant amount of O or N on the carbon.[12,13] In addition, the surface modification is generally not sustainable because of the use of expensive chemicals, large energy footprint, and required waste disposal during and after treatment.

Here, we present N-functionalization of AC through an efficient, sustainable, low-cost, and potentially scalable method with "soft nitriding" by low temperature heating of AC and urea. Urea is a N-rich and readily available chemical that can be potentially reused from urine waste, and it is ideal for N-functionalization of AC. Pd dispersion was significantly improved on N-functionalized AC, in contrast to native AC, and Pd on N-functionalized AC promoted nitrite and bromate hydrogenation kinetics, represented by first-order reaction rate constants and turnover frequency (TOF). However, these catalysts inhibited chlorite and chlorate hydrogenation kinetics, suggesting that different mechanisms may determine the reactivity of oxyanion hydrogenation. A scheme of preparing Pd nanoparticle catalysts is shown in Scheme 1. Our study highlights (i) a strategy for catalyst development and application and (ii) catalysts should be tailored for a specific reaction to achieve optimum performance, though the

Received: October 29, 2018
Accepted: December 6, 2018
Published: December 6, 2018

DOI: 10.1021/acsanm.8b01949
ACS Appl. Nano Mater. XXXX, XXX, XXX−XXX

Scheme 1. Low-Temperature Urea Treatment, Also Known as "Soft Nitriding", of Activated Carbon (AC) for the Synthesis of N-Functionalized AC and Pd Nanocatalysts

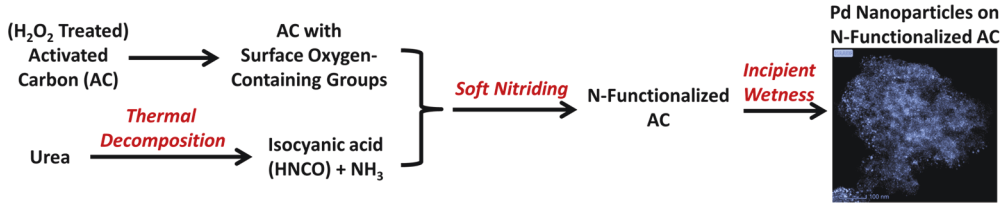

Table 1. Bulk and Surface Elemental Content Analysis for AC Supports and Pd Catalysts and Calculated Pd Dispersion

	bulk elemental content by the CHN analysis (wt %)			surface elemental content by the XPS analysis (at %, ~<10 nm)				bulk Pd by ICP-MS (wt %)	
sample	C	H	N	C	O	N	Pd	Pd	Pd dispersion (%)[a]
AC	89.0 ± 0.0	0.2 ± 0.0	0.3 ± 0.1	96.5	3.5	0.0			
OAC	85.7 ± 0.0	0.1 ± 0.1	0.3 ± 0.1	91.3	8.4	0.3			
NAC1.5	71.0 ± 0.1	0.9 ± 0.1	13.6 ± 0.2	71.5	8.9	19.6			
NOAC1.5	70.0 ± 0.1	1.0 ± 0.1	13.9 ± 0.1	67.3	9.8	23.0			
Pd/AC[b]	85.3 ± 0.6	0.2 ± 0.0	0.5 ± 0.1	86.1	9.8	1.0	3.1	4.1	7.3
Pd/OAC[b]	83.6 ± 0.1	0.1 ± 0.1	0.5 ± 0.0	86.5	10.4	1.0	2.0	3.9	16.9
Pd/NAC1.5[b]	81.4 ± 0.5	0.1 ± 0.1	3.0 ± 0.1	72.5	18.7	2.8	6.1	4.9	12.1
Pd/NOAC1.5[b]	79.6 ± 0.0	0.1 ± 0.0	3.1 ± 0.0	75.2	16.3	3.5	5.0	4.9	24.6

[a]See the Supporting Information (SI) for the calculation of Pd dispersion. [b]Pd was loaded via incipient wetness and subsequent thermal treatment in N_2 and H_2.

oxyanions were believed to have similar properties and behaviors.

Low-temperature urea treatment of AC (150 °C for 2 h and then 300 °C for additional 2 h in N_2, see details in the Supporting Information (SI)) grafts N-functional groups onto the surface of carbon (the prepared samples are NAC*x*, where *x* is the mass ratio of urea to AC), mainly through the reaction between NH_3 and HNCO generated from the thermal decomposition of urea and the surface O-containing sites (e.g., carboxylic and hydroxyl groups) of AC (Scheme 1), also known as "soft nitriding".[14] We also treated AC with 35 wt % H_2O_2 under a mild condition (50 °C for 5 h, see details in the SI) prior to nitriding to increase the number of O-containing sites and prepare OAC,[11] and consequently to increase N-loading of OAC (by treating OAC at 150 °C for 2 h and then 300 °C for additional 2 h in N_2, see details in the SI; the prepared samples are NOAC*x*, where *x* is the mass ratio of urea to OAC). Based on the elemental content analysis by X-ray photoelectron spectroscopy (XPS) for surface AC (analyzed depth <10 nm, Table 1), OAC showed an increased O content compared to AC (8.4 vs 3.5 at %), NAC1.5 and NOAC1.5 exhibited a substantially increased N content compared to AC (19.6 and 23.0 v 0.0 at %) and H_2O_2 treatment improved the extent of nitriding, in agreement with the previous study.[14,15] NAC1.5 and NOAC1.5 showed an increased O content compared to AC (8.9 and 9.8 vs 3.5 at %), likely due to the decomposition of urea grafting some O-containing sites to AC. The bulk elemental content (Table 1), characterized by the CHN analysis, also revealed that NAC1.5 and NOAC1.5 had a significantly higher amount of N compared to AC (13.6 ± 0.2 and 13.9 ± 0.1 vs 0.3 ± 0.1 wt %). The N/C molar ratio was significantly higher on the surface than in the bulk (comparison between XPS and CHN results, Table S1), indicating that nitriding was favored at the AC surface.[16] However, substantial reduction of N contents was observed after Pd loading via incipient wetness and subsequent thermal treatment in N_2 and H_2 (300 °C for 2 h in N_2 and additional 2 h in H_2; Pd/support represents the catalyst prepared under this condition without further notification), and Pd/NAC1.5 and Pd/NOAC1.5 only had 2.8 and 3.5 at % of N on the catalyst surface and 3.0 ± 0.1 and 3.1 ± 0.0 wt % of N in the bulk catalyst (Table 1). N-functional groups in NAC1.5 and NOAC1.5 were not thermally stable and they partially decomposed in the heating process for Pd loading.[13,16] The conclusion was also supported by the BET analysis that a substantial increase in the surface area and pore volume was observed after Pd loading (NAC1.5 vs Pd/NAC1.5, Table S2).[13] Interestingly, a slight increase of the bulk and surface N content was also observed for AC and OAC after Pd loading (Table 1), possibly due to the precursor $Pd(NO_3)_2$ introducing N during catalyst preparation. Surface O content was similar for Pd/AC and Pd/OAC (9.8 vs 10.4 at %), but much higher for Pd/NAC1.5 and Pd/NOAC1.5 (18.7 vs 16.3 at %), as indicated by XPS. H_2O_2 treatment might be too mild to introduce thermally stable O-functional groups to the AC.

The oxidation state and bonding environment of the supports and catalysts were characterized by XPS (Figure 1). It is not clear from the XPS data what type of new product was present (if any) on the catalyst support surface after calcination, with respect to N and O species. For NAC1.5 and NOAC1.5, there was measurably high amounts of O (8.9−9.8 at %) that had a slightly sharper O peak centered around 532.1 eV (most likely organic C−O species or C═O species), as well as high N (19.6−23.0 at %) centered around 400.0 eV (most likely products from the urea treatment).[14,17] These results most likely indicate decomposition products from urea occupied the surface of the support, which could also be confirmed by the fact that NAC1.5 showed a significant lower surface area compared with AC (Table S2). Every other sample analyzed (AC, OAC, Pd/AC, Pd/OAC, Pd/NAC1.5, and Pd/NOAC1.5) showed similarly shaped, broad O peaks, with little definition, and centered around 532.5 eV. This is

DOI: 10.1021/acsanm.8b01949
ACS Appl. Nano Mater. XXXX, XXX, XXX−XXX

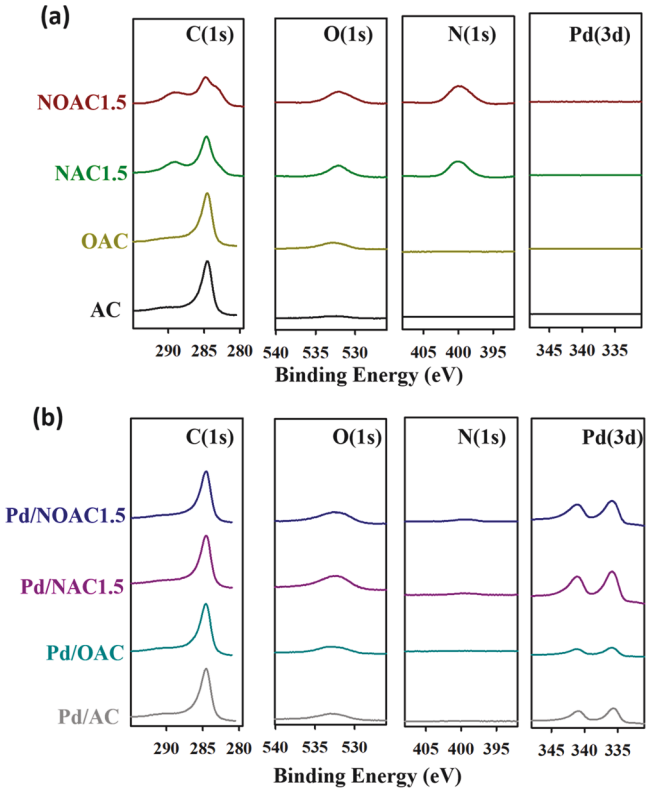

Figure 1. X-ray photoelectron spectroscopy (XPS) of (a) AC, OAC, NAC1.5, and NOAC1.5 and (b) Pd/AC, Pd/OAC, Pd/NAC1.5, and Pd/NOAC1.5.

likely some O bonded to the AC support. However, inspection of the C region for all of the catalysts containing Pd (i.e., C 1s of each sample reduced under H_2) clearly showed that each catalyst support was almost complete graphitic (i.e., C 1s region ~284.5 eV).[18] Although there was additional O (at %) measured on these catalyst samples, because the nature of the C 1s did not change significantly, we conclude this O could be the result of the unreacted precursor, and/or decomposed carbonaceous species from the urea coadditive used to treat the AC support. Regarding the N that was bonded to each of the catalyst supports, the two AC catalyst samples not treated with N-containing precursor (i.e., Pd/AC and Pd/OAC) had 1.0 at % N. The other two samples (i.e., Pd/NAC1.5 and Pd/NOAC1.5) had 2.8 and 3.5 at % N, respectively. While this very slight increase in N content on the catalyst support surface (1.8−2.5 at % increase) could be due to a new N species bonded to the AC surface, however the XPS was not able to discern what that species might be. The C 1s regions of these samples appear no different than the other catalysts (they all appeared graphitic). The main conclusion we could make is that both treatments (O- or N-functionalization) altered the intermediate surface of the AC support in some manner to facilitate some improved ability for the support to receive Pd and bind more strongly. Higher surface Pd content on these samples for Pd/NAC1.5 and Pd/NOA1.5 could potentially lead to higher reactivity, in contrast to Pd/AC and Pd/OAC. It is a stretch to suppose but perhaps the decomposition products themselves were the primary catalyst support, and they somehow incorporated themselves into the AC upon reduction of the Pd.[13,14]

Both NOAC1.5 and NAC1.5 showed significantly different peak shapes for the C 1s region, which could not be identified but most likely represented either (1) intermediate decomposition products of the urea-AC reaction or (2) modification of the AC surface. These other features were a peak at ~289.0 eV (indicating C in a higher oxidation state, that is, C═O), and a slight shoulder on the lower binding energy side (indicating some of the reduced form of C on the surface).[14] Since these features were present in the sample not treated with an oxidizing agent (NAC1.5), as well as the sample treated with oxidizing agent (NOAC1.5), it seems more likely that the reason for these features were from intermediate decomposition products of the urea−AC reaction, which were eventually reduced and departed from the AC surface after loading Pd during the incipient wetness and subsequent thermal treatment in N_2 and H_2 (these spectral featured disappeared in each of the samples containing Pd).

Pd nanoparticles were uniform distributed across NAC1.5 and NOAC1.5, with an average diameter of 4.0 ± 1.2 and 2.9 ± 0.9 nm, respectively, and only small agglomerations were occasionally observed (Figures 2 and S1). The average Pd nanoparticle size of Pd/AC (5.6 ± 2.3 nm) and Pd/OAC (4.7 ± 2.4 nm) was slightly larger and agglomerates of Pd particles were present (Figures 2 and S1), as indicated in Pd nanoparticle size histograms. AC itself has a high surface area, however, it decreased significantly after loading Pd (Pd/AC in Table S2), which might indicate that Pd nanoparticles have been successfully loaded inside the pores of the AC, accompanying by a noticeable decrease in pore volume (Table S2). In addition, Pd dispersion of Pd/NOAC1.5 was about 3.4-fold higher than that of Pd/AC (7.3% vs 24.6% in Table 1), which also supports the presence of smaller Pd nanoparticles and more uniform Pd distribution on Pd/NOAC1.5. N-functional groups can act as basic coordination sites and facilitate anchoring small Pd nanoparticles via electrostatic interactions.[13,14] Our results further confirm that N-functionalization is helpful to stabilize small Pd nanoparticles on carbon supports and thus promotes Pd dispersion. The high-resolution transmission electron microscopy (HRTEM) (Figure S2) confirmed the presence of Pd(0) metal nanoparticles, with the Pd (111) lattice spacing of ~0.22 nm, consistent with XPS results (the presence of Pd($3d_{5/2}$/$3d_{3/2}$) doublet and the Pd($3d_{5/2}$) binding energy of 335.2 (±0.1) eV, Figure 1b). The elemental distribution of all catalysts was also characterized by high angle annular dark field-scanning transmission electron microscopy (HAADF-STEM) and energy-dispersive X-ray spectroscopy (EDX) (Figures S3−S6). Pd nanoparticle distribution was more uniform on N-functionalized and H_2O_2 treated AC supports, in contrast to the native AC support. Uniform N distribution on Pd/NAC1.5 and Pd/NOAC1.5 was also observed, which further confirms the effectiveness of N-functionalization of AC by "soft nitriding" (Figures S5 and S6). Pd was observed to accumulate more on the support surface than in the bulk (Table S3), consistent with our previous findings.[18,19] N-functionalization further promotes the accumulation of Pd on the support surface (Table S3), likely due to AC pore blockage by urea decomposition intermediates in "soft nitriding" that prevents Pd precursor infiltration or an increased N content on the support surface that facilitates Pd coordination and binding.

In our preliminary experiments, we prepared a series of catalysts with different synthesis methods (i.e., wet impregnation, ethylene glycol (EG) reduction, and incipient wetness)

DOI: 10.1021/acsanm.8b01949
ACS Appl. Nano Mater. XXXX, XXX, XXX−XXX

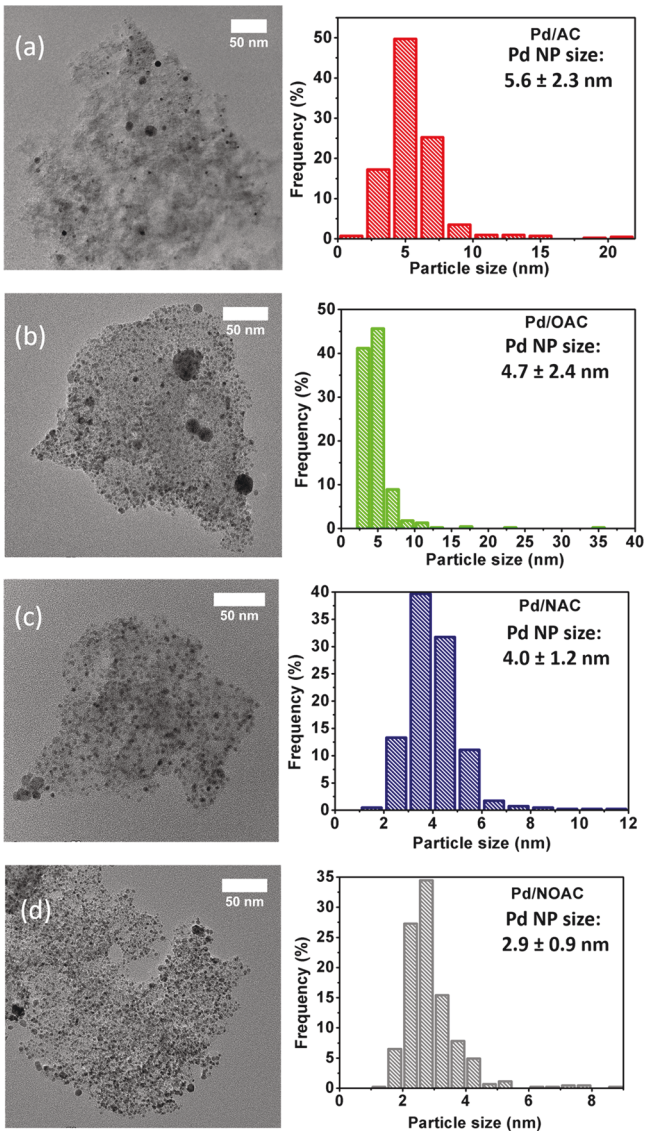

Figure 2. Transmission electron microscopy (TEM) and Pd nanoparticle (NP) size distribution of (a) Pd/AC, (b) Pd/OAC, (c) Pd/NAC1.5, and (d) Pd/NOAC1.5. Pd was loaded via incipient wetness and subsequent thermal treatment in N_2 and H_2.

(Figure S7) and tested catalyst performance for nitrite hydrogenation. In contrast to previous studies,[13,14] wet impregnation of both cationic and anionic Pd precursors (i.e., $Pd(NO_3)_2$ and Na_2PdCl_4) on functionalized AC did not generate Pd catalysts with significantly improved reactivity, compared with the Pd catalysts on native AC (Figures S7a and S7b). In our own work, EG reduction was proven to be an excellent method for preparing high reactivity Pd-based catalysts supported on graphitic carbon nitrides.[20] Nevertheless, EG reduction did not work for most of the functionalized AC, except for the Pd on OAC (Figure S7c). Compared to the other synthesis procedures, incipient wetness is promising because it significantly improved catalytic activity for nitrite hydrogenation: the pseudo-first-order reaction rate constant enhanced by 1.6, 4.8, and 6.3 fold on Pd/OAC, Pd/NAC1.5, and Pd/NOAC1.5 when compared to Pd/AC (Figure S7d). Compared with Pd/NAC1.5, an increased mass ratio of urea to AC in "soft nitriding" or tandem treatment of AC with urea did not promote reactivity (Pd/NAC3, Pd/NAC1.5−2, and Pd/NOAC1.5−2, catalyst annotation details in the SI), because the incomplete thermal decomposition of excess urea possibly blocked AC pores and thus lowered the accessibility of Pd nanoparticles to the support. Therefore, our study focuses on the Pd catalysts (i.e., Pd/AC, Pd/OAC, Pd/NAC1.5, and Pd/NOAC1.5) synthesized by incipient wetness and subsequent thermal treatment in N_2 and H_2 because of their optimum catalytic performance.

Four common oxyanion contaminants were selected to evaluate the catalytic performance in hydrogenation. Nitrite is a reduction intermediate of nitrate, which comes from extensive agricultural practices and fertilizer applications, whereas bromate, chlorite, and chlorate are disinfection byproducts. U.S. EPA has regulated the maximum contaminant level for nitrite, bromate, and chlorite in the drinking water as 1 (as N), 0.01, and 1 mg L^{-1}, respectively.[21] Here, we report the hydrogenation rate constants for these oxyanions on native and functionalized AC supported Pd catalysts, that is, pseudo-first-order reaction rate constants normalized to the bulk mass loading of Pd (details in the SI). For nitrite hydrogenation, the hydrogenation rate constant was enhanced significantly from 16.5 ± 5.6, to 26.7 ± 8.3, to 64.7 ± 6.8, and to 86.7 ± 6.5 L min^{-1} (g of bulk Pd)$^{-1}$ for Pd/AC, Pd/OAC, Pd/NAC1.5, and Pd/NOAC1.5, respectively (Figure 3a). This enhanced catalytic activity could be ascribed to the small Pd nanoparticle sizes (Figure 2) and high Pd dispersion (Table 1) resulting from N-functionalization of the carbon support. In addition to the overall reactivity represented by the hydrogenation rate constant, we also report the intrinsic reactivity that is characterized by the initial turnover frequency (TOF_0). TOF_0 evaluates the number of contaminant molecules reduced per exposed Pd site per minute at the beginning of a reaction, and the details of calculation are included in the SI. N-functionalization also improved the TOF_0 for nitrite hydrogenation (28.9 ± 9.9 min^{-1} for Pd/AC and 20.2 ± 6.3 min^{-1} for Pd/OAC vs 68.6 ± 7.2 min^{-1} for Pd/NAC1.5 and 45.1 ± 3.4 min^{-1} for Pd/NOAC1.5). These results are in contrast with previous studies showing that the TOF_0 for nitrite hydrogenation by CNF supported Pd catalysts was constant, despite different Pd nanoparticle sizes and Pd dispersion,[4,22] suggesting factors other than Pd dispersion or nanoparticle size determine the intrinsic catalytic activity for nitrite hydrogenation. N-functionalization could enhance the accessibility of oxyanions to Pd sites due to increased hydrophilicity and basicity of the supports, strengthen metal−support interactions by altering catalyst electronic properties, and improve the adsorption of reactants and intermediates on the catalysts.[4,12,16,22−26] TOF_0 for nitrite hydrogenation on native and functionalized AC supported catalysts could be positively correlated with surface Pd loading compared to the bulk (Table S3), which might indicate mass transfer limited reaction kinetics. Pd closer to the AC surface does not need extensive diffusion of reactants for the reaction. We evaluated external and intraparticle mass transfer rates in nitrite hydrogenation, and both mass transfer processes could limit reaction kinetics (see the SI). It is not surprising because AC has a highly porous and tortuous structure with abundant micropores and is relatively large in the particle size (100 mesh, corresponding to ∼149 μm). The zeta potential of Pd/OAC was more negative compared to the other catalysts (Figure S8), which was measured under the same ionic strength and pH as the reaction solution (1 mM of electrolyte, pH 5.0), and the electrostatic repulsion between anionic nitrite and the

DOI: 10.1021/acsanm.8b01949
ACS Appl. Nano Mater. XXXX, XXX, XXX−XXX

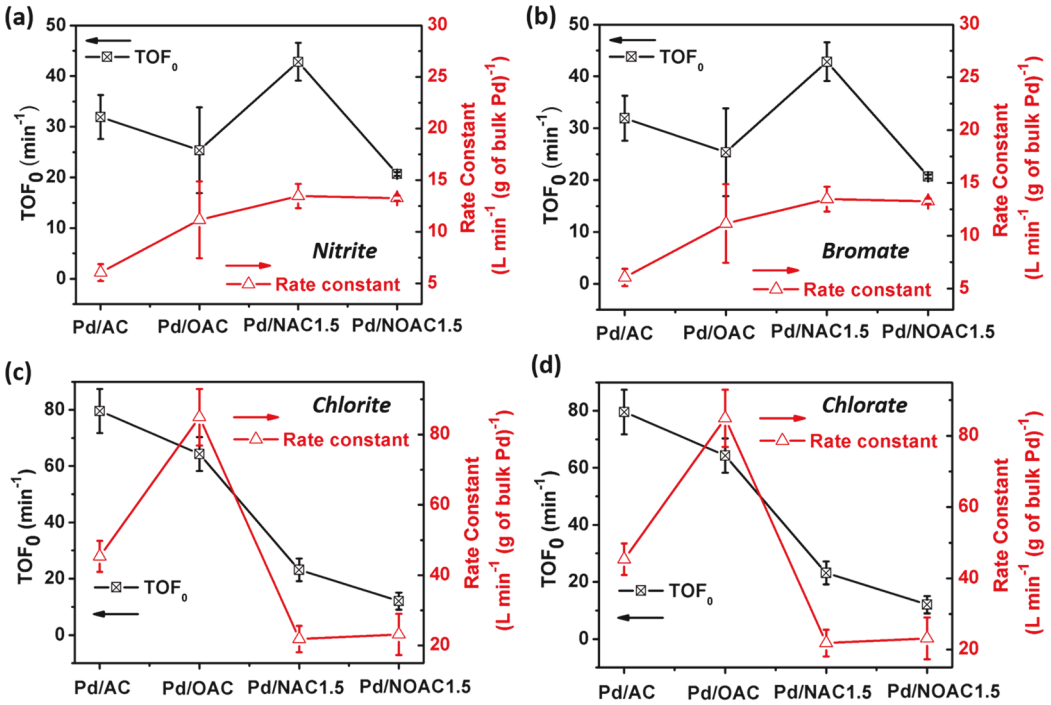

Figure 3. Reaction rate constants and initial turnover frequency (TOF_0) for the hydrogenation of (a) nitrite, (b) bromate, (c) chlorite, and (d) chlorate. Error bars represent the standard deviation of replicates.

negatively charged support could partially explain the observed TOF_0.[5,14] We speculate that the increased intrinsic reactivity for Pd/NAC1.5 and Pd/NOAC1.5 may also result from the increase of spillover of reactive atomic hydrogen (H_{ads}) because of N-functionalization. Hydrogen spillover is defined as the dissociative chemisorption of hydrogen on metal nanoparticles and subsequent migration of the H_{ads} to adjacent surfaces of the support. Hydrogen spillover has been observed in Ru catalysts supported on N-doped carbon and in hydrogenation reactions.[27,28] Therefore, hydrogen spillover could also occur on these N-functionalized AC-supported Pd catalysts, and it could promote nitrite hydrogenation kinetics.

The reaction rate constant for bromate hydrogenation was also enhanced for N-functionalized and H_2O_2 treated AC compared to native AC, similar to nitrite hydrogenation, which could also be attributed to improved Pd dispersion for Pd/OAC, Pd/NAC1.5, and Pd/NOAC1.5. However, only TOF_0 of Pd/NAC1.5 was statistically larger than that of Pd/AC, and the result did not provide a strong argument that N-functionalization enhanced intrinsic reactivity for bromate hydrogenation. Moreover, TOF_0 of Pd/NOAC1.5 is even lower than that of Pd/AC for bromate hydrogenation. Comparing Pd/NAC1.5 with Pd/NOAC1.5 and Pd/AC with Pd/OAC, it seems that O-functionalization of the support inhibited the TOF_0 for both nitrite and bromate hydrogenation (Figures 3a and 3b), though Pd dispersion, surface area, and pore volume (Tables 1 and S2) of Pd/NAC1.5 and Pd/AC were comparably lower than those of Pd/NOAC1.5 and Pd/OAC, respectively. We speculate that O-functionalization could influence electronic properties of Pd nanoparticles, as well as consequent binding of contaminants to Pd and reactivity of the contaminants on Pd.[28−30]

Surprisingly, the hydrogenation kinetics of chlorite and chlorate on Pd catalysts showed significantly different trends compared to nitrite and bromate hydrogenation (Figures 3c and 3d). N-functionalization significantly lowered chlorite hydrogenation rate constants but did not change chlorate hydrogenation rate constants compared to Pd/AC, though far more Pd sites were exposed for contaminant hydrogenation (Table 1). Moreover, Pd residing closer to the support surface for N-functionalized AC catalysts that was believed to increase the mass transfer rate did not promote the overall reactivity. In addition, the zeta potential of the catalysts cannot explain the trend for both chlorite and chlorate hydrogenation (Figure S8). In terms of TOF_0, Pd/AC and Pd/OAC outperformed other catalysts for chlorite and chlorate hydrogenation, respectively. Catalysts with N-functionalized supports showed notably lower intrinsic reactivity (in TOF_0) for both chlorite and chlorate hydrogenation, suggesting that N-functionalization could poison Pd catalysts in contaminant hydrogenation, possibly due to the strong binding of Pd by N-containing species, which block active sites for chlorite and chlorate hydrogenation.[31−33] Chlorate hydrogenation was conducted at pH 3.0 in contrast to the hydrogenation of nitrite, bromate, and chlorite at pH 5.0, since negligible reactivity was observed at higher pH for chlorate (data not shown). These results suggest different mechanisms determine oxyanion hydrogenation kinetics on Pd catalysts, though all oxyanions seem to share similar properties and behaviors (e.g., same negative charge). Very limited study has focused on chlorite and chlorate on Pd catalysts to date, and further exploration is needed. One possible explanation is that reduced availability of H^+ limits chlorite and chlorate hydrogenation kinetics in Pd catalysis. H^+ might bind to N-functional groups (e.g., amine protonation), and it cannot be used for oxygen atom transfer to facilitate deoxygenation of chlorite or chlorate (a similar mechanism highlighted the important role of H^+ for perchlorate hydrogenation[34]). Also, the active sites responsible for catalytic hydrogenation may differ among these oxyanions tested in this study.[29]

DOI: 10.1021/acsanm.8b01949
ACS Appl. Nano Mater. XXXX, XXX, XXX−XXX

Our study provides an efficient, sustainable, low-cost, and potentially scalable method to tailor AC supports for Pd-based catalysis with improved performance for water purification. Compared to other conventional and emerging catalyst supports, AC is the still most widely accepted and used in industrial practice. "Soft nitriding" with urea at low temperature was used to functionalize AC with N-containing groups, and catalysts prepared via incipient wetness on these tailored AC supports showed a significantly enhanced reactivity for nitrite and bromate hydrogenation by hydrogen gas. The enhanced reactivity could be attributed to an increased number of surface Pd(0) sites, improved accessibility of oxyanions to Pd sites (e.g., higher hydrophilicity and basicity of the supports, promoted adsorption and mass transfer of oxyanions), altered catalyst electronic properties, and hydrogen spillover. As pointed out by previous studies, one major technical barrier for implementing Pd-based catalysis for oxyanion hydrogenation in engineering practices is the low catalytic activity and associated high cost of Pd.[29] Life cycle assessment for Pd-based catalysis also suggested that increasing the catalytic activity would significantly lower adverse environmental impacts of oxyanion hydrogenation (i.e., perchlorate).[35] Our study could have significant impacts in the field of catalytic hydrogenation for water purification, by providing industrially viable catalysts for engineering applications.

In addition to practical applications, our study also sheds light on understanding Pd-based catalysis for oxyanion hydrogenation. N-functionalization had dramatically different impacts on the intrinsic hydrogenation kinetics of nitrite, bromate, chlorite, and chlorate, though all of the contaminants are oxyanions with one negative charge. N-functionalization of AC improved nitrite and bromate hydrogenation kinetics, but inhibited chlorite and chlorate hydrogenation kinetics. Our study highlights the design of Pd-based catalysts for water purification should be *contaminant specific*, and we cannot generalize one golden rule for catalyst design and implementation for the removal of all contaminants.

■ ASSOCIATED CONTENT

Supporting Information

The Supporting Information is available free of charge on the ACS Publications website at DOI: 10.1021/acsanm.8b01949.

Experimental details of catalyst synthesis and characterization, contaminant hydrogenation experiments, and evaluation of mass transfer limitations (PDF)

■ AUTHOR INFORMATION

Corresponding Author

*Phone: 202-994-0506. Fax: 202-994-0127. E-mail: danmengshuai@gwu.edu. Website: http://materwatersus.weebly.com/.

ORCID

Tao Ye: 0000-0003-4768-1811
Maocong Hu: 0000-0002-2726-5979
Michael J. Wagner: 0000-0001-9559-7804
Danmeng Shuai: 0000-0003-3817-4092

Notes

The authors declare no competing financial interest.

■ ACKNOWLEDGMENTS

We acknowledge National Science Foundation grant CBET-1437989 and Dewberry Fellowship (for T.Y.) from the Department of Civil and Environmental Engineering at The George Washington University (GW). We thank Likun Hua and Prof. Wen Zhang in the Department of Civil and Environmental Engineering at New Jersey Institute of Technology for zeta potential analyses.

■ REFERENCES

(1) Wada, K.; Hirata, T.; Hosokawa, S.; Iwamoto, S.; Inoue, M. Effect of Supports on Pd−Cu Bimetallic Catalysts for Nitrate and Nitrite Reduction in Water. *Catal. Today* **2012**, *185*, 81−87.

(2) Yoshinaga, Y.; Akita, T.; Mikami, I.; Okuhara, T. Hydrogenation of Nitrate in Water to Nitrogen over Pd−Cu Supported on Active Carbon. *J. Catal.* **2002**, *207*, 37−45.

(3) Soares, O. S. G. P.; Órfão, J. J. M.; Pereira, M. F. R. Pd−Cu and Pt−Cu Catalysts Supported on Carbon Nanotubes for Nitrate Reduction in Water. *Ind. Eng. Chem. Res.* **2010**, *49*, 7183−7192.

(4) Shuai, D.; Choe, J. K.; Shapley, J. R.; Werth, C. J. Enhanced Activity and Selectivity of Carbon Nanofiber Supported Pd Catalysts for Nitrite Reduction. *Environ. Sci. Technol.* **2012**, *46*, 2847−2855.

(5) Ye, T.; Durkin, D. P.; Hu, M.; Wang, X.; Banek, N. A.; Wagner, M. J.; Shuai, D. Enhancement of Nitrite Reduction Kinetics on Electrospun Pd-Carbon Nanomaterial Catalysts for Water Purification. *ACS Appl. Mater. Interfaces* **2016**, *8*, 17739−17744.

(6) Rodríguez-reinoso, F. The Role of Carbon Materials in Heterogeneous Catalysis. *Carbon* **1998**, *36*, 159−175.

(7) Soares, O. S. G. P.; Órfão, J. J. M.; Pereira, M. F. R. Activated Carbon Supported Metal Catalysts for Nitrate and Nitrite Reduction in Water. *Catal. Lett.* **2008**, *126*, 253−260.

(8) Soares, O. S. G. P.; Órfão, J. J. M.; Pereira, M. F. R. Bimetallic Catalysts Supported on Activated Carbon for the Nitrate Reduction in Water: Optimization of Catalysts Composition. *Appl. Catal., B* **2009**, *91*, 441−448.

(9) Soares, O. S. G. P.; Órfão, J. J. M.; Pereira, M. F. R. Nitrate Reduction Catalyzed by Pd−Cu and Pt−Cu Supported on Different Carbon Materials. *Catal. Lett.* **2010**, *139*, 97−104.

(10) Mikami, I.; Sakamoto, Y.; Yoshinaga, Y.; Okuhara, T. Kinetic and Adsorption Studies on the Hydrogenation of Nitrate and Nitrite in Water Using Pd-Cu on Active Carbon Support. *Appl. Catal., B* **2003**, *44*, 79−86.

(11) Radkevich, V. Z.; Senko, T. L.; Wilson, K.; Grishenko, L. M.; Zaderko, A. N.; Diyuk, V. Y. The Influence of Surface Functionalization of Activated Carbon on Palladium Dispersion and Catalytic Activity in Hydrogen Oxidation. *Appl. Catal., A* **2008**, *335*, 241−251.

(12) Li, M.; Xu, F.; Li, H.; Wang, Y. Nitrogen-Doped Porous Carbon Materials: Promising Catalysts or Catalyst Supports for Heterogeneous Hydrogenation and Oxidation. *Catal. Sci. Technol.* **2016**, *6*, 3670−3693.

(13) Li, Z.; Yang, X.; Tsumori, N.; Liu, Z.; Himeda, Y.; Autrey, T.; Xu, Q. Tandem Nitrogen Functionalization of Porous Carbon: Toward Immobilizing Highly Active Palladium Nanoclusters for Dehydrogenation of Formic Acid. *ACS Catal.* **2017**, *7*, 2720−2724.

(14) Liu, B.; Yao, H.; Song, W.; Jin, L.; Mosa, I. M.; Rusling, J. F.; Suib, S. L.; He, J. Ligand-Free Noble Metal Nanocluster Catalysts on Carbon Supports via "Soft" Nitriding. *J. Am. Chem. Soc.* **2016**, *138*, 4718−4721.

(15) Jia, Y. F.; Xiao, B.; Thomas, K. M. Adsorption of Metal Ions on Nitrogen Surface Functional Groups in Activated Carbons. *Langmuir* **2002**, *18*, 470−478.

(16) Nie, R.; Jiang, H.; Lu, X.; Zhou, D.; Xia, Q. Highly Active Electron-Deficient Pd Clusters on N-Doped Active Carbon for Aromatic Ring Hydrogenation. *Catal. Sci. Technol.* **2016**, *6*, 1913−1920.

(17) Burg, P.; Fydrych, P.; Cagniant, D.; Nanse, G.; Bimer, J.; Jankowska, A. The Characterization of Nitrogen-Enriched Activated

DOI: 10.1021/acsanm.8b01949
ACS Appl. Nano Mater. XXXX, XXX, XXX−XXX

Carbons by IR, XPS and LSER Methods. *Carbon* **2002**, *40*, 1521−1531.
(18) Durkin, D. P.; Ye, T.; Larson, E. G.; Haverhals, L. M.; Livi, K. J. T.; De Long, H. C.; Trulove, P. C.; Fairbrother, D. H.; Shuai, D. Lignocellulose Fiber- and Welded Fiber- Supports for Palladium-Based Catalytic Hydrogenation: A Natural Fiber Welding Application for Water Treatment. *ACS Sustainable Chem. Eng.* **2016**, *4*, 5511−5522.
(19) Durkin, D. P.; Ye, T.; Choi, J.; Livi, K. J. T.; Long, H. C. D.; Trulove, P. C.; Fairbrother, D. H.; Haverhals, L. M.; Shuai, D. Sustainable and Scalable Natural Fiber Welded Palladium-Indium Catalysts for Nitrate Reduction. *Appl. Catal., B* **2018**, *221*, 290−301.
(20) Ye, T.; Durkin, D. P.; Banek, N. A.; Wagner, M. J.; Shuai, D. Graphitic Carbon Nitride Supported Ultrafine Pd and Pd−Cu Catalysts: Enhanced Reactivity, Selectivity, and Longevity for Nitrite and Nitrate Hydrogenation. *ACS Appl. Mater. Interfaces* **2017**, *9*, 27421−27426.
(21) U.S. EPA. National Primary Drinking Water Regulations: Stage 2. Disinfectants and Disinfection By-Products Rule: Final Rule. *Fed. Reg.* **2006**, *71*, 388.
(22) Chinthaginjala, J. K.; Bitter, J. H.; Lefferts, L. Thin Layer of Carbon-Nano-Fibers (CNFs) as Catalyst Support for Fast Mass Transfer in Hydrogenation of Nitrite. *Appl. Catal., A* **2010**, *383*, 24−32.
(23) Chen, L.; Cooper, A. C.; Pez, G. P.; Cheng, H. Mechanistic Study on Hydrogen Spillover onto Graphitic Carbon Materials. *J. Phys. Chem. C* **2007**, *111*, 18995−19000.
(24) Zhou, Y.; Neyerlin, K.; Olson, T. S.; Pylypenko, S.; Bult, J.; Dinh, H. N.; Gennett, T.; Shao, Z.; O'Hayre, R. Enhancement of Pt and Pt-Alloy Fuel Cell Catalyst Activity and Durability *via* Nitrogen-Modified Carbon Supports. *Energy Environ. Sci.* **2010**, *3*, 1437−1446.
(25) Xi, J.; Xie, C.; Zhang, Y.; Wang, L.; Xiao, J.; Duan, X.; Ren, J.; Xiao, F.; Wang, S. Pd Nanoparticles Decorated N-Doped Graphene Quantum Dots@N-Doped Carbon Hollow Nanospheres with High Electrochemical Sensing Performance in Cancer Detection. *ACS Appl. Mater. Interfaces* **2016**, *8*, 22563−22573.
(26) Xi, J.; Sun, H.; Wang, D.; Zhang, Z.; Duan, X.; Xiao, J.; Xiao, F.; Liu, L.; Wang, S. Confined-Interface-Directed Synthesis of Palladium Single-Atom Catalysts on Graphene/Amorphous Carbon. *Appl. Catal., B* **2018**, *225*, 291−297.
(27) Wang, L.; Yang, F. H.; Yang, R. T. Hydrogen Storage Properties of B- and N-Doped Microporous Carbon. *AIChE J.* **2009**, *55* (7), 1823−1833.
(28) Wang, Y.; Liu, J.; Wang, P.; Werth, C. J.; Strathmann, T. J. Palladium Nanoparticles Encapsulated in Core−Shell Silica: A Structured Hydrogenation Catalyst with Enhanced Activity for Reduction of Oxyanion Water Pollutants. *ACS Catal.* **2014**, *4* (10), 3551−3559.
(29) Chaplin, B. P.; Reinhard, M.; Schneider, W. F.; Schüth, C.; Shapley, J. R.; Strathmann, T. J.; Werth, C. J. Critical Review of Pd-Based Catalytic Treatment of Priority Contaminants in Water. *Environ. Sci. Technol.* **2012**, *46*, 3655−3670.
(30) Chen, P.; Yang, F.; Kostka, A.; Xia, W. Interaction of Cobalt Nanoparticles with Oxygen- and Nitrogen-Functionalized Carbon Nanotubes and Impact on Nitrobenzene Hydrogenation Catalysis. *ACS Catal.* **2014**, *4*, 1478−1486.
(31) Motoyama, Y.; Lee, Y.; Tsuji, K.; Yoon, S. H.; Mochida, I.; Nagashima, H. Platinum Nanoparticles Supported on Nitrogen-doped Carbon Nanofibers as Efficient Poisoning Catalysts for the Hydrogenation of Nitroarenes. *ChemCatChem* **2011**, *3*, 1578−1581.
(32) Lee, Y.; Motoyama, Y.; Tsuji, K.; Yoon, S. H.; Mochida, I.; Nagashima, H. (Z)-Selective Partial Hydrogenation of Internal Alkynes by Using Palladium Nanoparticles Supported on Nitrogen-Doped Carbon Nanofiber. *ChemCatChem* **2012**, *4*, 778−781.
(33) Chen, P.; Chew, L. M.; Xia, W. The Influence of the Residual Growth Catalyst in Functionalized Carbon Nanotubes on Supported Pt Nanoparticles Applied in Selective Olefin Hydrogenation. *J. Catal.* **2013**, *307*, 84−93.
(34) Hurley, K. D.; Shapley, J. R. Efficient Heterogeneous Catalytic Reduction of Perchlorate in Water. *Environ. Sci. Technol.* **2007**, *41*, 2044−2049.
(35) Choe, J. K.; Mehnert, M. H.; Guest, J. S.; Strathmann, T. J.; Werth, C. J. Comparative Assessment of the Environmental Sustainability of Existing and Emerging Perchlorate Treatment Technologies for Drinking Water. *Environ. Sci. Technol.* **2013**, *47*, 4644−4652.

DOI: 10.1021/acsanm.8b01949
ACS Appl. Nano Mater. XXXX, XXX, XXX−XXX